

See discussions, stats, and author profiles for this publication at: <https://www.researchgate.net/publication/372595705>

# A Convergent Neural Network for Non-Blind Image Deblurring

Conference Paper · July 2023

DOI: 10.1109/ICIP49359.2023.10222656

---

CITATIONS

4

---

READS

265

5 authors, including:



Yanan Zhao

Nanyang Technological University

10 PUBLICATIONS 80 CITATIONS

SEE PROFILE

# A CONVERGENT NEURAL NETWORK FOR NON-BLIND IMAGE DEBLURRING

Yanan Zhao<sup>1</sup>, Yuelong Li<sup>2</sup>, Haichuan Zhang<sup>3</sup>, Vishal Monga<sup>3</sup>, Yonina C. Eldar<sup>4</sup>

<sup>1</sup>School of Electrical and Electronic Engineering, Nanyang Technological University, Singapore,

<sup>2</sup>Amazon, Sunnyvale, CA, USA

<sup>3</sup>Department of Electrical Engineering, Pennsylvania State University, USA

<sup>4</sup>Faculty of Mathematics and Computer Science, Weizmann Institute of Science, Israel

## ABSTRACT

In recent years, algorithm unrolling has emerged as a powerful technique for designing interpretable neural networks based on iterative algorithms. Imaging inverse problems have particularly benefited from unrolling based deep network design since many traditional model-based approaches rely on iterative optimization. Despite exciting progress, typical unrolling approaches heuristically design layer-specific convolution weights to improve performance. Crucially, convergence properties of the underlying iterative algorithm are lost once layer specific parameters are learned from training data. In this paper, we propose a neural network architecture that breaks the trade-off between retaining algorithm properties while simultaneously enhancing performance. We focus on non-blind image deblurring problem and unroll the widely-applied Half-Quadratic Splitting (HQS) algorithm. We develop a new parameterization scheme that enforces the layer-specific parameters to asymptotically approach certain fixed points, a new result that we analytically establish. Experimental results show that our approach outperforms many state of the art non-blind deblurring techniques on benchmark datasets, while enabling convergence and interpretability.

**Index Terms**— Image deblurring, Algorithm unrolling, deep neural networks.

## 1. INTRODUCTION

Image deconvolution refers to the process of recovering a sharp image from a recorded image corrupted by blur and noise. Image deconvolution consists of blind and non-blind image deconvolution. The task of blind image deconvolution is to recover the sharp image given only the blurry image, without knowing the blur kernels [1–4]. Non-blind image deconvolution, where precise knowledge of the blur kernels are assumed known a priori, continues to be an interesting topic despite decades of algorithmic developments. In this work, we concentrate on the non-blind image deblurring problem with the particular case of motion deblurring due to camera shaking when conducting experimental studies. Nevertheless, our formulation and analysis are versatile across blur kernels.

Due to the low-pass nature of the blur kernels, recovering the sharp latent image from blurry samples is an ill-posed problem. One effective way to address this is to incorporate prior models of natural images [5, 6]. More recent methods focus on either modelling the statistics of image gradients [7, 8] or imposing sparsity constraints over the transform coefficients [9, 10]. All aforementioned techniques hinge on analytic or handcrafted prior models, which may not faithfully fit real data distributions. Therefore, many works strive to learn prior models from real data [11]. While being more effective than the conventional gradient sparsity priors, these methods are typically slow.

Complementary to the aforementioned approaches, deep neural networks have become the mainstream approach in learning-based methods [12, 13]. Another line of research applies pre-deconvolution techniques. Rather than feeding the original blurry images into the network directly, one can obtain a deconvolved image by deblurring it with a simple deconvolution algorithm such as a Wiener filter, and then input the deconvolved image into a network to perform artifact removal [14–17].

While deep learning is empirically successful with sufficient training data, a major drawback is that it usually sacrifices interpretability, as the deep networks are typically constructed by stacking common layers rather than derived from physical mechanisms. Gregor *et al.* [18, 19] develop a sparse coding technique called algorithm unrolling which could be regarded as a bridge between traditional iterative algorithms and modern deep neural networks, and hence offer promise in filling the interpretability gap. Passing through the network is equivalent to executing the iterative algorithm a finite number of times, and the trained network can be naturally interpreted as a parameter optimized network. In recent years, there is a growing trend of research along this route in various imaging fields [20, 21]. However, to ensure good performance in practice, the network layers deviate from the original iterations in that layer-specific parameters are adopted, leaving the convergence guarantee at questions. Similar issues also persists in other unrolling works [22], where customizations of the layers are incorporated, and convergence guarantees for unrolled

network has hence become a common open question.

From an algorithmic perspective, HQS is a generic and widely applied technique for solving prior-based non-blind image deblurring. The convergence of conventional HQS has been established in [23], where strong convergence properties for the algorithm is derived including finite convergence for certain variables. Nevertheless, their analysis is restricted to the scenarios where the parameters are fixed per iterations, and hence cannot be directly applied to many unrolling approaches where the parameters are altered.

In this paper, we propose deep interpretable neural network called DCUNBD by unrolling the widely-applied HQS algorithm with a new parametrization scheme that ensures convergence while simultaneously retaining the practical benefits. By experimental comparison with state-of-the-art deblurring techniques, DCUNBD achieves a favorable gain of PSNR by about 1 dB and a SSIM of 0.1 over both traditional iterative algorithms and modern deep neural networks.

## 2. DEEP, CONVERGENT, UNROLLED HALF-QUADRATIC SPLITTING

### 2.1. Half-Quadratic Splitting Algorithm for Non-blind deblurring

Assuming the camera motion is purely translational and the scene is planar (ignoring the depth variations), image blurring can be modelled as a discrete convolution process:  $\mathbf{y} = \mathbf{k} * \mathbf{u} + \mathbf{n}$ , where  $\mathbf{y} \in \mathbb{R}^m$  denotes the observations of the signal  $\mathbf{u} \in \mathbb{R}^n$ , received from a system with impulse response  $\mathbf{k} \in \mathbb{R}^k$  and  $\mathbf{n} \in \mathbb{R}^m$  is a noise modelled as Gaussian. In non-blind deblurring, it is assumed that  $k$  is pre-determined and the goal is to solve for  $\mathbf{u}$ . The total variation minimization approach in gradient domain reduces to solving the following convex optimization problem:

$$\min_{\mathbf{u} \in \mathbb{R}^n} \frac{\mu}{2} \|\mathbf{y} - \mathbf{K}\mathbf{u}\|_2^2 + \|\mathbf{D}_x \mathbf{u}\|_1 + \|\mathbf{D}_y \mathbf{u}\|_1, \quad (1)$$

where  $\mathbf{K} \in \mathbb{R}^{m \times n}$  is the Toeplitz matrix corresponding to the convolution kernel  $\mathbf{k}$ , and  $\mathbf{D}_x, \mathbf{D}_y \in \mathbb{R}^{n \times n}$  are the gradient operators which capture horizontal and vertical image gradients, respectively, and  $\mu > 0$  is a regularization parameter that controls the strength of enforcing gradient sparsity. A widely employed algorithm for solving (1) is the Half-Quadratic Splitting (HQS) algorithm [23]. By introducing auxiliary variables  $\mathbf{w}_x, \mathbf{w}_y \in \mathbb{R}^n$  as surrogates of image gradients, (1) can be cast into the following constrained minimization problem:

$$\begin{aligned} \min_{\mathbf{u}, \mathbf{w}_x, \mathbf{w}_y \in \mathbb{R}^n} & \frac{\mu}{2} \|\mathbf{y} - \mathbf{K}\mathbf{u}\|_2^2 + \|\mathbf{w}_x\|_1 + \|\mathbf{w}_y\|_1 \\ & + \frac{\beta}{2} (\|\mathbf{D}_x \mathbf{u} - \mathbf{w}_x\|_2^2 + \|\mathbf{D}_y \mathbf{u} - \mathbf{w}_y\|_2^2), \end{aligned} \quad (2)$$

where  $\beta > 0$  is a parameter controlling the relaxation strength. The HQS algorithm proceeds by minimizing over  $\mathbf{u}$  and  $\mathbf{w}_x, \mathbf{w}_y$  in an alternating fashion. A desirable property

of (2) is that each sub-problem (over  $\mathbf{u}$  or over  $\mathbf{w}$ ) admits closed-form solutions, enabling to express the iteration steps analytically for  $l = 1, 2, \dots$ :

$$\begin{aligned} \mathbf{M} & \leftarrow \sum_{i \in x, y} \mathbf{D}_i^T \mathbf{D}_i + \frac{\mu}{\beta} \mathbf{K}^T \mathbf{K}, \\ \mathbf{u}^l & \leftarrow \mathbf{M}^{-1} \left( \sum_{i \in x, y} \mathbf{D}_i^T \mathbf{w}_i^l + \frac{\mu}{\beta} \mathbf{K}^T \mathbf{y} \right) \\ \mathbf{w}_x^{l+1} & \leftarrow s_{\frac{1}{\beta}}(\mathbf{D}_x \mathbf{u}^l), \quad \mathbf{w}_y^{l+1} \leftarrow s_{\frac{1}{\beta}}(\mathbf{D}_y \mathbf{u}^l), \end{aligned} \quad (3)$$

where  $s_\lambda$  is the soft-thresholding operator defined element-wise as  $s_\lambda(x) = \text{sgn}(x) \cdot \max\{|x| - \lambda, 0\}$ .

### 2.2. Deep Unrolled Half-Quadratic Splitting

In conventional HQS iterations (3), the operators  $\mathbf{D}_x, \mathbf{D}_y$ , or their underlying gradient filters, are determined analytically. The parameters  $\beta, \mu$  are also chosen as fixed values. In practice, better filters and parameters can be learned from real datasets through end-to-end training to improve performance. As discussed in [18], for a particular iterative algorithm, each iteration step can be considered as one layer of a network, and executing the iterative steps corresponds to concatenating these layers together to form a deep network. In this way, the HQS algorithm is unrolled into a deep network, which we can train end-to-end to optimize the filters and parameters.

Therefore, we further generalize HQS by adopting different parameters  $\mathbf{D}_x^l, \mathbf{D}_y^l, \beta^l$  per layer. In addition, for each layer we use  $C$  filters instead of two, i.e., we embed  $\{\mathbf{D}_i^l\}_{i=1}^C$  into each layer. With these generalizations, each network layer now comprises the following iterations:

$$\mathbf{M}^l \leftarrow \mathbf{D}^{lT} \mathbf{D}^l + \frac{\mu}{\beta^l} \mathbf{K}^T \mathbf{K}, \quad (4)$$

$$\mathbf{u}^l \leftarrow \mathbf{M}^{l-1} \left( \mathbf{D}^{lT} \mathbf{w}^l + \frac{\mu}{\beta^l} \mathbf{K}^T \mathbf{y} \right), \quad (5)$$

$$\mathbf{w}^{l+1} \leftarrow s^l(\mathbf{D}^l \mathbf{u}^l), \quad (6)$$

where  $\mathbf{w}^l = [\mathbf{w}_1^{lT}, \mathbf{w}_2^{lT}, \dots, \mathbf{w}_C^{lT}]^T$ ,  $s^l(\cdot) = s_{\frac{1}{\beta^l}}(\cdot)$  and  $\mathbf{D}^l = [\mathbf{D}_1^l, \mathbf{D}_2^l, \dots, \mathbf{D}_C^l]^T$ . Furthermore, define  $h^l(\mathbf{w}^l) = \mathbf{D}^l \mathbf{u}^l$ , we can then express the iterations succinctly as  $\mathbf{w}^{l+1} = s^l(h^l(\mathbf{w}^l))$ .

### 2.3. Deep Convergent Unrolled for Non-blind Deblurring

With the mappings  $s^l, h^l$  defined, the unrolled network can be visually depicted as a diagram in Fig. 1. Compared to traditional HQS, unrolled HQS performs much better in practice thanks to its enriched set of parameters [3]; furthermore, it typically executes merely tens of layers in practice, as opposed to hundreds of thousands of iterations, and is usually much more computationally efficient than HQS. However, since  $\mathbf{D}^l$  and  $\beta^l$  are layer specific parameters learned with

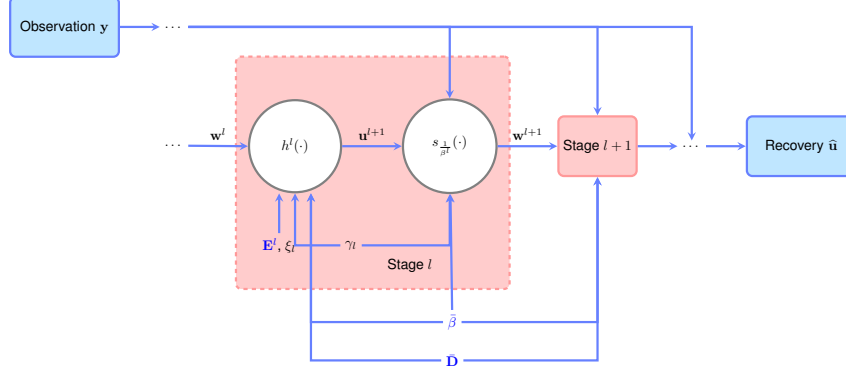


**Fig. 1:** Diagram of the proposed DCUNBD network. Trainable parameters are colored in blue.

training data, the convergence guarantee for HQS no longer holds; additionally, interpretability might be undermined because the unrolled network, when having infinitely many layers, may no longer converge to a particular fixed point. Nevertheless, under certain conditions, if both the filters and the parameters are asymptotically fixed, i.e., both converge to certain fixed values, then the convergence guarantee could be preserved. In [23], convergence is established for fixed  $\mathbf{D}$ ,  $\mu$  and  $\beta$ , where the mappings  $s$  and  $h$  are fixed per iteration. However, in unrolled HQS, the fixed point of  $s^l \circ h^l$  is not defined. We hypothesize that, if  $\{\mathbf{D}^l\}_l$  and  $\{\beta^l\}_l$  are convergent sequences, i.e.,  $\lim_{l \rightarrow \infty} \mathbf{D}^l = \bar{\mathbf{D}}$  and  $\lim_{l \rightarrow \infty} \beta^l = \bar{\beta}$ , then  $\{\mathbf{w}^l\}_l$  converges to a fixed point of  $s^* \circ h^*$ , with  $s^*, h^*$  being the asymptotic mappings of  $s^l$  and  $h^l$ , respectively. In particular, we propose the following parameterization:

$$\mathbf{D}^l = \bar{\mathbf{D}} + \xi_l \mathbf{E}^l, \quad \beta^l = \bar{\beta} + \gamma_l, \quad (7)$$

where  $\xi_l$  and  $\gamma_l$  are both real vanishing sequences with  $\lim_{l \rightarrow \infty} \xi_l = 0$  and  $\lim_{l \rightarrow \infty} \gamma_l = 0$ , and  $\bar{\mathbf{D}}, \mathbf{E}^l$  are both Toeplitz matrices representing discrete convolutions, and  $\mathbf{E}^l$  is norm-bounded. Since  $\mathbf{E}^l$ 's are different across layers, the number of parameters for  $\mathbf{D}^l$  does not decrease due to this parameterization scheme, which enables the unrolled network to have great modeling power. In practice,  $\bar{\mathbf{D}}$  and  $\mathbf{E}^l$ 's are learned from real data whereas  $\xi_l$  and  $\gamma_l$  are chosen sequences. In [23], convergence is established for fixed  $\mathbf{D}$ ,  $\mu$  and  $\beta$ , where the mappings  $s$  and  $h$  are fixed per iteration. However, in unrolled HQS, the fixed point of  $s^l \circ h^l$  is not defined. We hypothesize that, if  $\{\mathbf{D}^l\}_l$  and  $\{\beta^l\}_l$  are convergent sequences, i.e.,  $\lim_{l \rightarrow \infty} \mathbf{D}^l = \bar{\mathbf{D}}$  and  $\lim_{l \rightarrow \infty} \beta^l = \bar{\beta}$ , then  $\{\mathbf{w}^l\}_l$  converges to a fixed point of  $s^* \circ h^*$ , with  $s^*, h^*$  being the asymptotic mappings of  $s^l$  and  $h^l$ , respectively. Then, the unrolled HQS network is formed as a deep interpretable convergent neural network architecture dubbed Deep Convergent Unrolling for Non-blind Deblurring (DCUNBD). The key analytical result we establish is that of the convergence of DCUNBD, which is formally stated below.

**Theorem 1. (Convergence result)** *For a fixed  $\mu > 0$ , under the parameterization given in (7), and suppose  $\xi_l \in \mathbb{R}$ ,  $\gamma_l \in \mathbb{R}$*

*are absolutely summable, meaning  $\sum_l |\xi_l|$  and  $\sum_l |\gamma_l|$  both converge. Furthermore, suppose that  $\{\mathbf{E}^l\}_l$  forms a bounded sequence, i.e.,  $\|\mathbf{E}^l\| \leq M$  for some  $M > 0$ . Then the sequence  $\{(\mathbf{w}^l, \mathbf{u}^l)\}$  generated by executing DCUNBD converges to  $\{(\mathbf{w}^*, \mathbf{u}^*)\}$  as  $l \rightarrow \infty$ .*  
*Proof.* See in [24].  $\square$

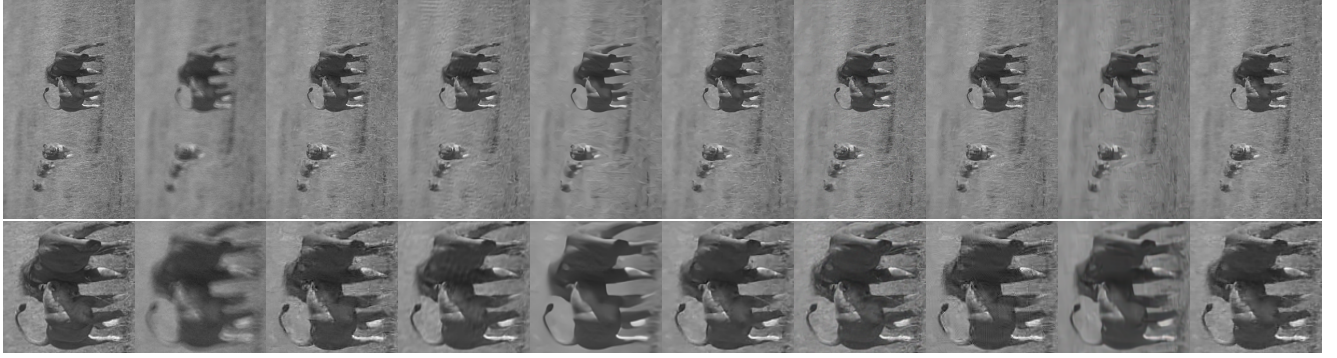
### 3. EXPERIMENTAL VALIDATION

We realize DCUNBD as a 30-layer network with a sequence of  $C = 4$  filters  $\mathbf{D}^l$ , with  $\xi_l = (0.5)^l$ ,  $\gamma_l = (0.5)^l$  and  $\bar{\mathbf{D}}, \mathbf{E}^l, \bar{\beta}$  are trainable model parameters. Further, via cross validation, we set the hyperparameter  $\mu = 5 \times 10^4$ .

**Training:** We use the Microsoft Common Objects in Context (MS COCO) dataset [28] as our training images. For training, 800 images were randomly selected and cropped to 424×424 pixels, and additionally 1000 realistic nonlinear kernels were generated using the method described in [20]. During each training step, we randomly select a batch of clear images and blur kernels from the training dataset, convolve each clear image with a blur kernel, and add Gaussian noise with a standard deviation of 1% to obtain the blurred and clear image pairs. Our training loss function is a combination of Mean Squared Error (MSE) and Mean Absolute Error (MAE). The Adam optimizer [29] with default settings is used to learn the network parameters  $\bar{\mathbf{D}}, \mathbf{E}^l, \bar{\beta}$ , and the learning rate is initialized at  $1 \times 10^{-3}$  and decreased by 5% after each epoch.

**Evaluation:** We used 100 images from the BSDS500 dataset [30] as test images to evaluate how methods adapt across datasets, and generated another 100 realistic nonlinear kernels using a recording camera motion trajectory (which did not overlap with training kernels) to generate the corresponding blurred images. We compare our results with state-of-the-art algorithms, including EPLL [11], BM3D [10], and SVD [17] (iterative algorithms with some learned components), and MLP [14], IRCNN [25], FCNN [26], and FNBD [27] (fully deep learning methods). The performance of these methods is evaluated using the Peak-Signal-to-Noise Ratio (PSNR) and Structural Similarity Index (SSIM) [31].

Sample test images and visual examples of reconstructed images from different methods are shown in Fig 2, and the



(a) Clear (b) Blurred (c) EPLL (d) MLP (e) IRCNN (f) FCNN (g) FNBD (h) BM3D (i) SVMAP (j) DCUNBD

**Fig. 2:** Visual comparison over BSD dataset and nonlinear kernels.

**Table 1:** Quantitative comparison over BSD dataset and nonlinear kernels. The best score is in bold fonts.

	<b>EPLL</b> [11]	<b>MLP</b> [14]	<b>IRCNN</b> [25]	<b>FCNN</b> [26]	<b>FNBD</b> [27]	<b>BM3D</b> [10]	<b>SVMAP</b> [17]	<b>DCUNBD</b>
SSIM	0.8812	0.8329	0.8309	0.8898	0.8793	0.8586	0.8880	<b>0.8985</b>
PSNR	29.3769	26.9809	28.3595	29.8539	29.5855	28.5916	28.7086	<b>30.2715</b>

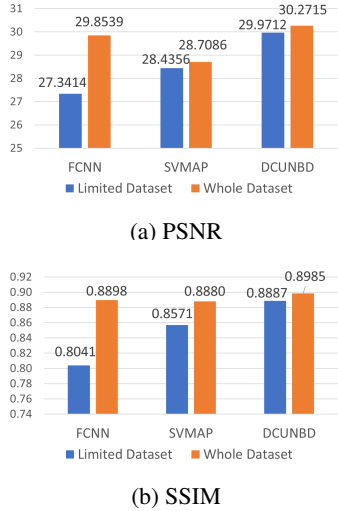


**Fig. 3:** Performance evaluation in a limited training set-up.

quantitative results are presented in Table 1. DCUNBD outperforms all competing methods, with the superior reconstruction of high-frequency details. It is followed by FCNN, while EPLL is the top-performing iterative algorithm. By zooming in on the elephant region in the sample image, shown in the second row of Fig 2, we compare the image detail reconstructed by all the methods. Due to EPLL’s processing on a patch level, the boundaries between patches may be noticeable in some areas. FCNN fails to produce the contrast in some regions. SVMAP produced the smoothest image among all the methods, but it also loses some detail. Overall the image processed by DCUNBD is closest to the original sharp image among all the competing methods.

We also test three methods with the highest score from the previous evaluation (FCNN, SVMAP, and DCUNBD) with

limited training conditions. These methods were trained on a limited dataset that only contains 10 % of the training images used for the results in Table 1. The test image set remains unchanged. The result is shown in fig 3. FCNN, a neural network with a large number of parameters, overfits when training is reduced, as its performance has a considerable drop on the limited dataset. SVMAP utilizes powerful image priors, which increases the method’s training robustness and shows a narrower gap between network trained on the whole dataset and the limited dataset. With the fewest parameters among the three methods, DCUNBD performs the best in a limited training scenario with the smallest gap (especially in SSIM) between the model trained on the limited dataset and the PSNR/SSIM scores for DCUNBD even in the face of limited training are higher than competing alternatives even as they have access to full training, i.e. DCUNBD demonstrates superior generalizability.

#### 4. CONCLUSION

This paper proposes a novel deep unrolling technique for the non-blind image deconvolution problem. We unroll the half-quadratic splitting (HQS) algorithm into a neural network structure that is interpretable. Key domain parameters such as image filters are no longer fixed to gradient choices as in traditional HQS but now learned through training data. As the main contribution, we develop a novel parametrization scheme that enforces structure on the learned parameters per layer in a manner that guarantees convergence of the designed unrolled network. Our proposal achieves a highly desirable balance between modeling power and desired analytical properties such as convergence enabling both performance gains in the sense of reconstructed image quality but also exhibits better generalizability in the face of limited training.

## 5. REFERENCES

- [1] D. Perrone and P. Favaro, “A clearer picture of total variation blind deconvolution,” *IEEE Trans. Pattern Anal. Mach. Intell.*, vol. 38, no. 6, pp. 1041–1055, Jun. 2016.
- [2] J. Pan, D. Sun, H. Pfister, and M. H. Yang, “Deblurring images via dark channel prior,” *IEEE Trans. Pattern Anal. Mach. Intell.*, vol. 40, no. 10.
- [3] Y. Li, M. Tofighi, J. Geng, V. Monga, and Y. C. Eldar, “Efficient and interpretable deep blind image deblurring via algorithm unrolling,” *IEEE Trans. on Comput. Imaging*, vol. 6, pp. 666–681, 2020.
- [4] Xianyu Ge, Jieqing Tan, Li Zhang, Jing Liu, and Dandan Hu, “Blind image deblurring with gaussian curvature of the image surface,” *Signal Process.: Image Commun.*, vol. 100, pp. 116531, 2022.
- [5] W. Norbert and M. Cybernéticien, *Extrapolation, interpolation, and smoothing of stationary time series: with engineering applications*, vol. 113, MIT press Cambridge, MA, 1949.
- [6] W. H. Richardson, “Bayesian-based iterative method of image restoration,” *J. Opt. Soc. Amer.*, vol. 62, no. 1, pp. 55–59, 1972.
- [7] A. Levin, Y. Weiss, F. Durand, and W.T. Freeman, “Understanding blind deconvolution algorithms,” *IEEE Trans. Pattern Anal. Mach. Intell.*, vol. 33, no. 12, pp. 2354–2367, Dec. 2011.
- [8] D. Krishnan and R. Fergus, “Fast image deconvolution using hyper-laplacian priors,” *Adv. Neural Inform. Process. Syst.*, vol. 22, 2009.
- [9] A. Danielyan, V. Katkovnik, and K. Egiazarian, “Bm3d frames and variational image deblurring,” *IEEE Trans. Image Process.*, vol. 21, no. 4, pp. 1715–1728, 2011.
- [10] Y. Mäkinen, L. Azzari, and A. Foi, “Collaborative filtering of correlated noise: Exact transform-domain variance for improved shrinkage and patch matching,” *IEEE Trans. Image Process.*, vol. 29, 2020.
- [11] D. Zoran and Y. Weiss, “From learning models of natural image patches to whole image restoration,” in *Int. Conf. Comput. Vis.* IEEE, 2011, pp. 479–486.
- [12] L. Xu, J. S.J. Ren, C. Liu, and J. Jia, “Deep convolutional neural network for image deconvolution,” in *Neural Inf. Process. Syst.*, 2014, pp. 1790–1798.
- [13] W. Ren, J. Zhang, L. Ma, J. Pan, X. Cao, W. Zuo, W. Liu, and M. Yang, “Deep non-blind deconvolution via generalized low-rank approximation,” *Adv. Neural Inform. Process. Syst.*, vol. 31, 2018.
- [14] C. J. Schuler, C. H. Burger, S. Harmeling, and B. Scholkopf, “A machine learning approach for non-blind image deconvolution,” in *Proc. IEEE Conf. Comput. Vis. Pattern Recognit.*, 2013, pp. 1067–1074.
- [15] R. Wang and D. Tao, “Training very deep cnns for general non-blind deconvolution,” *IEEE Trans. on Image Process.*, vol. 27, no. 6, pp. 2897–2910, 2018.
- [16] K. He, X. Zhang, S. Ren, and J. Sun, “Deep residual learning for image recognition,” in *Proc. IEEE Conf. Comput. Vis. Pattern Recognit.*, 2016, pp. 770–778.
- [17] J. Dong, S. Roth, and B. Schiele, “Learning spatially-variant map models for non-blind image deblurring,” in *Proc. IEEE Conf. Comput. Vis. Pattern Recognit.*, 2021, pp. 4886–4895.
- [18] K. Gregor and Y. LeCun, “Learning fast approximations of sparse coding,” in *Proc. 27th Int. Conf. Int. Conf. Mach. Learn.*, 2010, pp. 399–406.
- [19] V. Monga, Y. Li, and Y. C. Eldar, “Algorithm unrolling: Interpretable, efficient deep learning for signal and image processing,” *IEEE Signal Process. Magazine*, vol. 38, no. 2, pp. 18–44, 2021.
- [20] Y. Li, M. Tofighi, J. Geng, V. Monga, and Y. C. Eldar, “Efficient and interpretable deep blind image deblurring via algorithm unrolling,” *IEEE Trans. Comput. Imaging*, vol. 6, pp. 666–681, Jan. 2020.
- [21] Nir Shlezinger, Yonina C. Eldar, and Stephen P. Boyd, “Model-based deep learning: On the intersection of deep learning and optimization,” *IEEE Access*, vol. 10, pp. 115384–115398, 2022.
- [22] J. R. Hershey, J. Le Roux, and F. Weninger, “Deep unfolding: Model-based inspiration of novel deep architectures,” *arXiv preprint arXiv:1409.2574*, 2014.
- [23] Y. Wang, J. Yang, W. Yin, and Y. Zhang, “A new alternating minimization algorithm for total variation image reconstruction,” *SIAM J. Imaging Sci.*, vol. 1, no. 3, pp. 248–272, 2008.
- [24] “Technical report in support of DCUNBD,” <http://signal.ee.psu.edu/ICIP23.pdf>.
- [25] K. Zhang, W. Zuo, S. Gu, and L. Zhang, “Learning deep cnn denoiser prior for image restoration,” in *Proc. IEEE Conf. Comput. Vis. Pattern Recognit.*
- [26] J. Zhang, J. Pan, W. Lai, R. Lau, and M. Yang, “Learning fully convolutional networks for iterative non-blind deconvolution,” in *Proc. IEEE Conf. Comput. Vis. Pattern Recognit.*, 2017, pp. 3817–3825.
- [27] H. Son and S. Lee, “Fast non-blind deconvolution via regularized residual networks with long/short skip-connections,” in *IEEE Int. Conf. Comput. Photography*. IEEE, 2017, pp. 1–10.
- [28] T. Lin, M. Maire, S. Belongie, J. Hays, P. Perona, D. Ramanan, P. Dollár, and C. L. Zitnick, “Microsoft coco: Common objects in context,” in *European Conf. Comput. Vis.* Springer, 2014, pp. 740–755.
- [29] D. P. Kingma and J. Ba, “Adam: A method for stochastic optimization,” *arXiv preprint arXiv:1412.6980*, 2014.
- [30] P. Arbelaez, M. Maire, C. Fowlkes, and J. Malik, “Contour detection and hierarchical image segmentation,” *IEEE Trans. Pattern Anal. Mach. Intell.*, vol. 33, no. 5, pp. 898–916, May 2011.
- [31] Z. Wang, A.C. Bovik, H.R. Sheikh, and E.P. Simoncelli, “Image quality assessment: from error visibility to structural similarity,” *IEEE Trans. Image Process.*, vol. 13, no. 4, pp. 600–612, 2004.